

Configurational effects in the nonradiative 5D_2 – 5D_1 transition processes of Sm^{2+} in $\text{BaFCl}_x\text{Br}_{1-x}$ mixed crystals

Jiahua Zhang, Shihua Huang, Jiaqi Yu

Laboratory of Excited State Processes and Changchun Institute of Physics, Chinese Academy of Sciences, Changchun 130021, PR China

Received 23 December 1996; in final form 20 February 1997

Abstract

The nonradiative 5D_2 – 5D_1 transition processes of Sm^{2+} in $\text{BaFCl}_x\text{Br}_{1-x}$ mixed crystals are investigated by using spectroscopic techniques in the thermal range 15–110 K. We found that the Sm^{2+} centers in different local configurations have different nonradiative 5D_2 – 5D_1 transition rates due to the indirect processes which occur through the $4f^55d$ band as intermediary. This characteristic leads to the fact that the inhomogeneous spectral distribution is strongly temperature dependent. It is observed that the different nonradiative rates are caused by the different positions of the low-lying $4f^55d$ states of the Sm^{2+} ions in local configurations.

1. Introduction

Numerous papers have been devoted to the investigations on the nonradiative f – f transition processes of Sm^{2+} in alkaline earth fluoride and halofluoride lattices [1–7]. The processes have been found to include a direct multiphonon f – f transition and an indirect multiphonon f –(d)– f transition which occurs through the $4f^55d$ band as intermediary. Gacon and co-workers [6,7] performed measurements of the temperature dependence of the nonradiative 5D_2 – 5D_1 transition rates in $\text{BaFCl}:\text{Sm}^{2+}$ and obtained that the thermal activation upwards to the $4f^55d$ band is a dominant process causing thermal quenching of the 5D_2 level.

$\text{BaFCl}_x\text{Br}_{1-x}:\text{Sm}^{2+}$ mixed crystals were first prepared for high temperature spectral hole burning [8], which has a potential application in high density

optical storage. The energy level scheme of Sm^{2+} in this system was observed to be similar to that in BaFCl because $\text{BaFCl}_x\text{Br}_{1-x}$ has the same structure as BaFCl , which belongs to the PbFCl -type family, from the results of X-ray diffraction [9]. In $\text{BaFCl}_x\text{Br}_{1-x}:\text{Sm}^{2+}$ lattices, a Sm^{2+} ion replacing a Ba^{2+} ion is surrounded by five nearest halo-ligands Cl^- and Br^- ions which form 6 different clusters, $\text{Cl}_n\text{Br}_{5-n}$ ($n = 0, 1, \dots, 5$) [10]. Recently, Jaaniso et al. [11] developed a model to describe the inhomogeneous broadening of optical spectra in substitutionally disordered crystals, which was compared to the experimental f – f fluorescence spectra of Sm^{2+} in $\text{SrFCl}_x\text{Br}_{1-x}$ at 30 K. 12 different local configurations in the 6 clusters in $\text{SrFCl}_x\text{Br}_{1-x}:\text{Sm}^{2+}$ were observed in the fluorescence spectra and considered to describe the inhomogeneous spectral distributions.

We found in $\text{BaFCl}_x\text{Br}_{1-x}:\text{Sm}^{2+}$ that the Sm^{2+}

ions in different local configurations have largely different nonradiative 5D_2 – 5D_1 transition rates. This characteristic results in the inhomogeneous spectral distribution being strongly temperature dependent. An investigation of the configuration dependent nonradiative transition is important not only for understanding the fluorescence properties, but also for comprehending the spectral hole burning dynamics and spectral hole shape in this system. We have previously studied the temperature dependence of the fluorescence of Sm^{2+} in $BaFCl_{0.5}Br_{0.5}$ [12]. This focused on the average effect of the fluorescence intensity. The variation in the inhomogeneous spectral distribution with temperature due to configurational effects was not investigated in detail. This Letter presents a study of the configurational dependent nonradiative 5D_2 – 5D_1 transition processes in $BaFCl_xBr_{1-x}:Sm^{2+}$ using spectroscopic techniques.

2. Experimental

$BaFCl_xBr_{1-x}:Sm^{2+}$ samples with different values of the composition x were made by mixing different stoichiometric amounts of previously prepared BaF_2 , $BaCl_2$ and $BaBr_2$ all doped nominally with 1% SmF_3 . The ground mixtures were heated to 900°C under a H_2 reduction atmosphere and kept at this reaction condition for 2 h before being slowly cooled down. In measuring the fluorescence excitation spectra within the 7F_0 – 5D_2 transition, a tunable dye laser with laser linewidth of 0.2 cm^{-1} , pumped by a pulsed Quanta-Ray DCR-2A Nd:YAG with a repetition frequency of 10 Hz, was used to scan the 7F_0 – 5D_2 transition while the fluorescence from the 5D_2 – 7F_3 or 5D_1 – 7F_0 transition was monitored by a D330 spectrometer. The same dye laser was also used to perform two photon spectral hole burning. The duration of each pulse was 10 ns. In measuring the fluorescence spectra, a 337.1 nm line from a nitrogen laser or a 570 nm line from the dye laser was used as the excitation source. The fluorescence was detected by a Spex-1403 monochromator. In the measurements of both the excitation spectra and the fluorescence spectra, the signal was recorded 50 μs after each exciting pulse with a sampling time of 5 μs . Different temperatures were obtained by using a closed cycle refrigerator.

3. Results and discussion

It was in $BaFCl_{0.5}Br_{0.5}:Sm^{2+}$ that we first observed that Sm^{2+} centers have different nonradiative 5D_2 – 5D_1 transition rates. Fig. 1 shows the time decay patterns of the 5D_2 – 7F_3 and 5D_1 – 7F_0 transitions in $BaFCl_{0.5}Br_{0.5}:Sm^{2+}$ and $BaFCl:Sm^{2+}$ under selective excitation of the 5D_2 level at 77 K. Under these excitation conditions, the population of the 5D_1 level is completely from the 5D_2 level through nonradiative transition. Then an increase with a maximum occurring at time $t_{\text{max}} = [\tau_1\tau_2/(\tau_1 - \tau_2)]\ln(\tau_1/\tau_2)$ is expected and observed in $BaFCl:Sm^{2+}$ as shown in Fig. 1; The τ_1 and τ_2 are the lifetimes of the 5D_1 and 5D_2 levels, obtained from the tails of the decay patterns of the 5D_1 and 5D_2 levels, respectively. The obtained τ_1 and τ_2 in $BaFCl:Sm^{2+}$ at 77 K are 760 and 130 μs , respectively. They yield $t_{\text{max}} = 277\text{ }\mu\text{s}$, which is in agreement with the experimental result presented in Fig. 1. The obtained τ_1 and τ_2 in $BaFCl_{0.5}Br_{0.5}:Sm^{2+}$ at 77 K are 780 and 280 μs , respectively. They yield $t_{\text{max}} = 448\text{ }\mu\text{s}$. However, no increase was observed in the decay pattern of the 5D_1 – 7F_0 transition in $BaFCl_{0.5}Br_{0.5}:Sm^{2+}$. A reasonable explanation for this result is that the Sm^{2+} centers have a different nonradiative 5D_2 – 5D_1 transition rate due to an indirect process involving the $4f^55d$ band, and some Sm^{2+} centers have fast indirect processes. This ex-

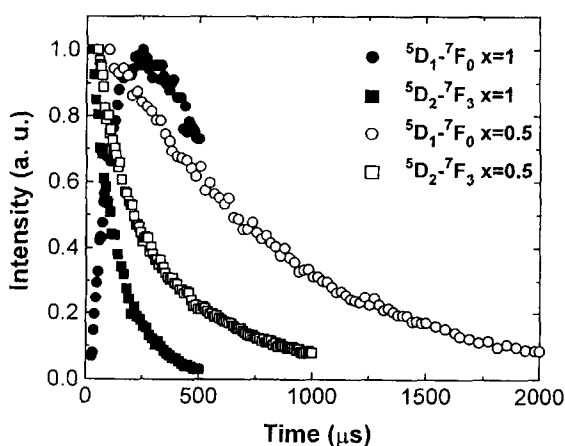


Fig. 1. The time decay patterns of the 5D_2 – 7F_3 and 5D_1 – 7F_0 transitions in $BaFCl:Sm^{2+}$ and $BaFCl_{0.5}Br_{0.5}:Sm^{2+}$ at 77 K under selective excitation of the 5D_2 level.

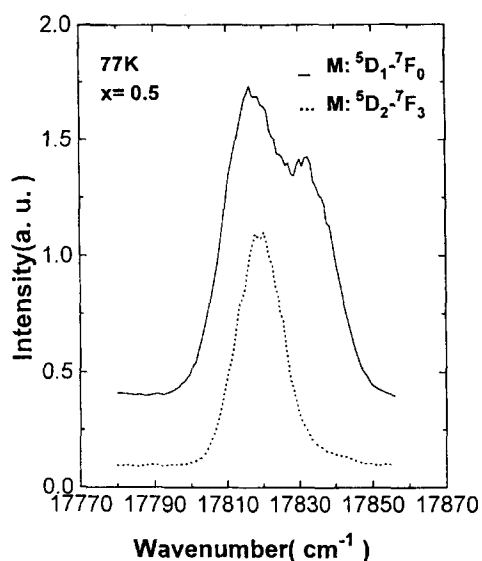


Fig. 2. Excitation spectra of the 7F_0 - 5D_2 transitions by monitoring (M) the 5D_2 - 7F_3 and 5D_1 - 7F_0 emissions of Sm^{2+} in $\text{BaFCl}_{0.5}\text{Br}_{0.5}$ at 77 K.

planation is based on the consideration that the Sm^{2+} ions are surrounded by different local configurations in this system [10,11], the 5d Stark states are subject to considerably larger crystal field effects than the 4f states [1,3,4], and the 5D_2 level is in the proximity of the low-lying 4f 5D_2 states [1,5–7]. In this case, the decay processes in $\text{BaFCl}_{0.5}\text{Br}_{0.5}:\text{Sm}^{2+}$ are described briefly as follows. The Sm^{2+} centers having faster nonradiative processes quickly relax to the 5D_1 states and those having slower nonradiative processes remain in the 5D_2 states after excitation of the 5D_2 level. In this way, the fact that no increase is observed in the decay pattern of 5D_1 corresponds to the faster centers, and the obtained decay pattern of 5D_2 corresponds to the slower centers. Therefore, the fluorescence from the 5D_2 and 5D_1 states originate from the slower and faster Sm^{2+} centers, respectively. These different Sm^{2+} centers can be separated in the excitation spectra within the 7F_0 - 5D_2 transitions when the 5D_2 - 7F_3 and 5D_1 - 7F_0 emissions are monitored, respectively. To separate these centers, we obtain the excitation spectra at 77 K by monitoring the 5D_2 - 7F_3 and 5D_1 - 7F_0 emissions, respectively, as shown in Fig. 2. The spectral distributions for 5D_2 - 7F_3 and 5D_1 - 7F_0 are clearly different. The spectrum for 5D_2 - 7F_3 presents one band,

while the spectrum for 5D_1 - 7F_0 presents two broad bands. These bands are attributed to the different local configurations in the $\text{Cl}_n\text{Br}_{5-n}$ clusters formed by 5 nearest neighboring Cl^- and Br^- ions around a Sm^{2+} ion according to an investigation of the inhomogeneous broadening of Sm^{2+} in $\text{MFCl}_x\text{Br}_{1-x}$ mixed crystals (M = Ba, Sr) [10,11]. Hence, the different spectral distributions shown in Fig. 2 are caused by the different local configurations having different nonradiative 5D_2 - 5D_1 transition rates. This assertion is also supported by the fact that no difference is observed between the excitation spectra of the 5D_2 - 7F_3 and 5D_1 - 7F_0 emissions in both the $\text{BaFCl}:\text{Sm}^{2+}$ and $\text{BaFBr}:\text{Sm}^{2+}$ systems.

In order to study the nonradiative processes of different local configurations, the excitation spectra are recorded at numerous temperatures between 15 and 110 K in $\text{BaFCl}_x\text{Br}_{1-x}:\text{Sm}^{2+}$ for $x = 0.8$ and

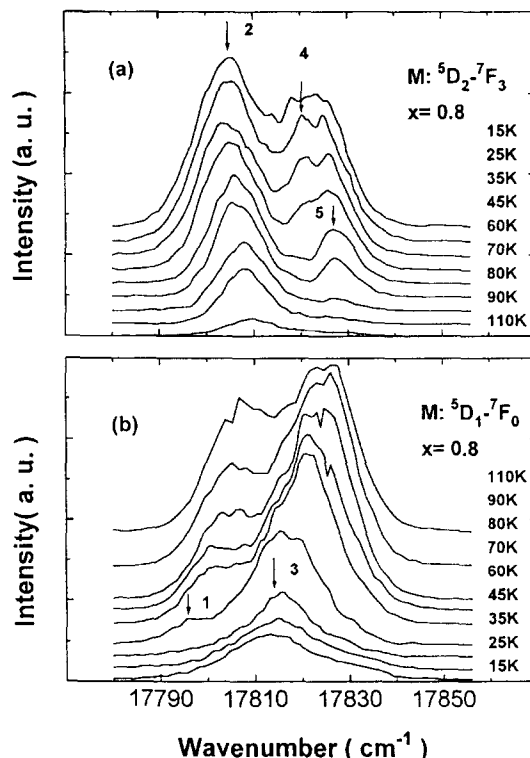


Fig. 3. Excitation spectra of the 7F_0 - 5D_2 transitions by monitoring (M) the 5D_2 - 7F_3 (a) and 5D_1 - 7F_0 (b) emissions of Sm^{2+} in $\text{BaFCl}_{0.8}\text{Br}_{0.2}$ at different temperatures. The cluster $\text{Cl}_n\text{Br}_{1-n}$ is labeled with 'n'.

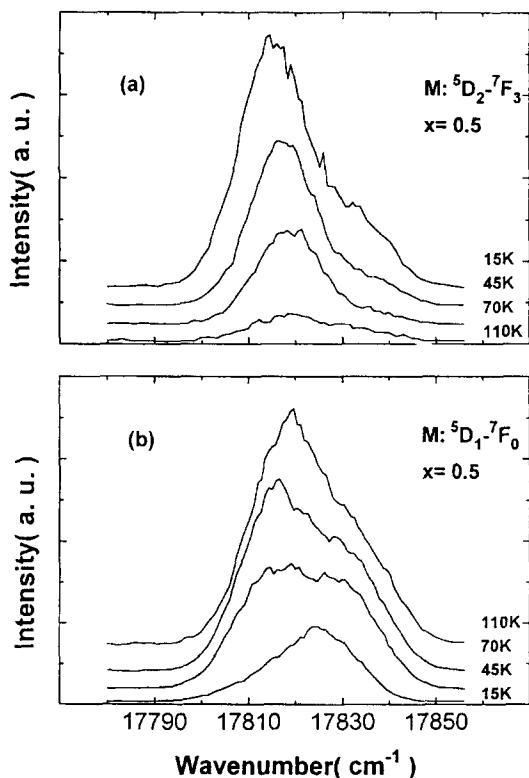


Fig. 4. Excitation spectra of the ${}^7F_0-{}^5D_2$ transitions by monitoring (M) the ${}^5D_2-{}^7F_3$ (a) and ${}^5D_1-{}^7F_0$ (b) emissions of Sm^{2+} in $\text{BaFCl}_{0.5}\text{Br}_{0.5}$ at different temperatures.

0.5, respectively, as shown in Figs. 3 and 4. The spectra show that the fluorescence intensity of ${}^5D_2-{}^7F_3$ decreases following the growth of ${}^5D_1-{}^7F_0$ emissions with the increase in temperature. This feature results from the nonradiative ${}^5D_2-{}^5D_1$ transition process. The behavior that the excitation spectra of ${}^5D_2-{}^7F_3$ and ${}^5D_1-{}^7F_0$ are different for each x , and that the spectral distributions change considerably with variations in temperature indicates different nonradiative ${}^5D_2-{}^5D_1$ transition rates in different configurations, which are frequency dependent.

In Fig. 3 the excitation spectra of ${}^5D_2-{}^7F_3$ and ${}^5D_1-{}^7F_0$ in $\text{BaFCl}_{0.8}\text{Br}_{0.2}:\text{Sm}^{2+}$ totally consist of five resolvable bands. According to the results of the investigation on the inhomogeneous broadening of optical spectra in $\text{SrFCl}_x\text{Br}_{1-x}:\text{Sm}^{2+}$ [11], the five bands in the spectra from the high energy side to the low-energy side mainly correspond to the configurations in the clusters $\text{Cl}_n\text{Br}_{5-n}$ with $n = 5, 4, 3, 2$ and

1, respectively. The cluster with $n=0$ is not observed at the low-energy side of the band $n=1$ because of the small number of this cluster for $x=0.8$. These different clusters are labeled with values of n , as shown in Fig. 3. In the spectra of $\text{BaFCl}_{0.5}\text{Br}_{0.5}:\text{Sm}^{2+}$ the different clusters cannot be resolved because the disorder of substitution reaches a maximum following the maximal band width for an individual configuration at $x=0.5$ [10,11]. The spectra presented in Figs. 3 and 4 show that the differences in the nonradiative ${}^5D_2-{}^5D_1$ transition rates in different configurations for the same composition x are large. Some configurations can completely relax from 5D_2 to 5D_1 and give fluorescence from 5D_1 even at 15 K, such as the $n=3$ band in Fig. 3(b). Some configurations remain in the 5D_2 states until a sufficiently high temperature. For instance, the $n=2$ band in Fig. 3(a) is quenched at 110 K. The different quenching temperatures of the 5D_2 levels may be due to the different positions of the low-lying $4f^55d$ states which are governed by local configurations. To examine this consideration, we measured the fluorescence spectra for different excitation wavelengths.

Fig. 5 shows the fluorescence spectra of the ${}^5D_2-{}^7F_0$ transition in $\text{BaFCl}_{0.8}\text{Br}_{0.2}:\text{Sm}^{2+}$ at 77 K on

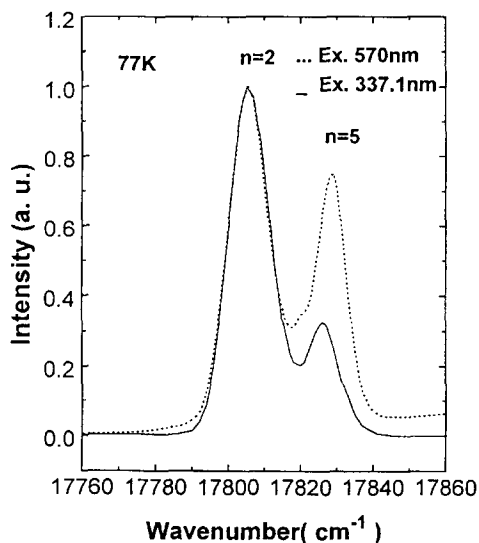


Fig. 5. Fluorescence spectra of the ${}^5D_2-{}^7F_0$ transitions in $\text{BaFCl}_{0.8}\text{Br}_{0.2}:\text{Sm}^{2+}$ at 77 K under 570 and 337.1 nm pulsed laser line excitations.

excitation of the $4f^55d$ band by 337.1 and 570 nm laser lines. The spectra exhibit a growth of the $n = 5$ band by using the 570 nm line instead of 337.1 nm line to excite the system. Considering that the 570 nm line excites the edge of the $4f^55d$ absorption band, the growth of the $n = 5$ band is interpreted as the low-lying $4f^55d$ states of the Cl_5Br_0 cluster being located at a lower position than the Cl_2Br_3 cluster. In this case, on one hand, the Cl_5Br_0 cluster is more effectively excited by the 570 nm line than the Cl_2Br_3 cluster, so the growth of the $n = 5$ band is expected; on the other hand, the Cl_5Br_0 cluster should have a smaller thermal activation energy than the Cl_2Br_3 cluster. This deduction has been supported by the fact that the quenching temperature of the $n = 5$ band is lower than that of the $n = 2$ band, as shown in Fig. 3(a). The fluorescence spectra for $x = 0.5$ and 0.25 are also measured under different excitation wavelengths. We obtain the same conclusion that the spectral distribution is dependent on the excitation wavelength, and the faster Sm^{2+} centers are in favor of a longer excitation wavelength. As a result, the positions of the low-lying $4f^55d$ states of the Sm^{2+} ions in different configurations are different, the faster centers have lower positions of the $4f^55d$ states.

To understand whether the configuration has an effect on the direct f–f transition rate of Sm^{2+} in $\text{BaFCl}_x\text{Br}_{1-x}:\text{Sm}^{2+}$. We performed the following experiments. We measured the time resolved excitation spectra of the ${}^5\text{D}_1\text{--}{}^7\text{F}_0$ emission within the ${}^7\text{F}_0\text{--}{}^5\text{D}_2$ transition at 120 K. At this temperature the ${}^5\text{D}_2$ level is quenched, the nonradiative transition from ${}^5\text{D}_2$ to ${}^5\text{D}_1$ is rapidly finished after the exciting pulse. Subsequently the ${}^5\text{D}_1$ level begins to decay without feeding from ${}^5\text{D}_2$. We found that the spectral distributions do not vary with delay times for each x . The experiment shows that the different configurations have the same lifetime of the ${}^5\text{D}_1$ level, i.e. the same radiative transition rate from ${}^5\text{D}_1$ to the ground state and the same ${}^5\text{D}_1\text{--}{}^5\text{D}_0$ direct multiphonon transition rate. In the ${}^5\text{D}_1\text{--}{}^5\text{D}_0$ nonradiative processes, the upward nonradiative transitions from ${}^5\text{D}_1$ to ${}^5\text{D}_2$ and the $4f^55d$ band can be neglected in the range of temperatures investigated because the energy gap between ${}^5\text{D}_2$ and ${}^5\text{D}_1$ is around 1940 cm^{-1} and that between the low-lying $4f^55d$ states and ${}^5\text{D}_1$ is larger than 1940 cm^{-1} .

Hence, the nonradiative ${}^5\text{D}_1\text{--}{}^5\text{D}_0$ process is determined by the direct process.

We have performed spectral hole burning in different configurations in the ${}^7\text{F}_0\text{--}{}^5\text{D}_2$ transitions under the same conditions. The same hole areas are probed in different configurations. This means that the radiative transition rate of the ${}^5\text{D}_2$ level is also configuration independent. The lifetimes of ${}^5\text{D}_2$, ${}^5\text{D}_1$ and ${}^5\text{D}_0$ for different x are measured at 15 K when the system is excited into the $4f^55d$ band by the 337.1 nm laser line. We observed that the lifetimes are almost unchanged with different x . It is worth stressing that the obtained lifetimes of ${}^5\text{D}_2$ correspond to slow centers in which the indirect processes can be neglected at 15 K, although the fast Sm^{2+} centers still have a large nonradiative ${}^5\text{D}_2\text{--}{}^5\text{D}_1$ transition rate at this temperature. From the experimental results mentioned above, we consider that the direct f–f transition rate is configuration and composition independent in $\text{BaFCl}_x\text{Br}_{1-x}:\text{Sm}^{2+}$. Under this condition, the fact that the excitation spectral distributions of ${}^5\text{D}_2\text{--}{}^7\text{F}_3$ and ${}^5\text{D}_1\text{--}{}^7\text{F}_0$ are different, as well as the spectral distribution being strongly temperature dependent definitely arises from the largely different indirect nonradiative ${}^5\text{D}_2\text{--}{}^5\text{D}_1$ transition rates for different local configurations.

4. Conclusions

The Sm^{2+} centers in different local configurations in $\text{BaFCl}_x\text{Br}_{1-x}$ have largely different nonradiative ${}^5\text{D}_2\text{--}{}^5\text{D}_1$ transition rates due to the different positions of the low-lying $4f^55d$ states. This characteristic leads to the fact that the inhomogeneous spectral distribution is strongly temperature dependent. The results of this study are helpful for probing the local environments of Sm^{2+} ions in $\text{MFCl}_x\text{Br}_{1-x}$ ($M = \text{Mg}, \text{Ca}, \text{Sr}, \text{Ba}$) mixed crystals and for comprehending the dephasing process and the spectral hole shape involved in the spectral hole burning of these systems.

Acknowledgements

The authors would like to thank Professor W. Qin and S. Lu for their valuable help in the experiment

and the data processing. This work was supported by the Project of the National Advanced Material Committee of China.

References

- [1] A.S.M. Mahbub'ul Alam, B. Di Bartolo, *J. Chem. Phys.* 47 (1967) 3790.
- [2] B. Birang, A.S.M. Mahbub'ul Alam, B. Di Bartolo, *J. Chem. Phys.* 50 (1969) 2750.
- [3] F.K. Fong, H.V. Lauer, C.R. Chilver, M.N. Miller, *J. Chem. Phys.* 63 (1975) 366.
- [4] H.V. Lauer Jr., F.K. Fong, *J. Chem. Phys.* 65 (1976) 3108.
- [5] J.C. Gacon, J.C. Souillat, J. Seriot, B. Di Bartolo, *Phys. Status Solidi A* 39 (1977) 147.
- [6] F. Gaume, J. C. Gacon, J. C. Souillat, J. Seriot, B. Di Bartolo, in *The Rare-Earths in Modern Science and Technology*, Plenum, New York, 1978.
- [7] J. C. Gacon, J. C. Souillat, J. Seriot, F. Gaume-Mahn, *J. Lumin.* 18/19 (1979) 244.
- [8] C. Wei, S. Huang, J. Yu, *J. Lumin.* 43 (1989) 161.
- [9] J. Lin, M. Su, *Chem. J. Chin. Univ.* 6 (1989) 957.
- [10] L. Zhang, J. Yu, S. Huang, *J. Lumin.* 45 (1990) 301.
- [11] R. Jaaniso, H. Hagemann, H. Bill, *J. Chem. Phys.* 101 (1994) 10323.
- [12] H. Song, J. Zhang, S. Huang, J. Yu, *J. Lumin.* 64 (1995) 189.